



**HAL**  
open science

## On-line loss and global efficiency simulation tool for electric vehicles applications

Charbel Zaghrini, Gabriel Khoury, Maurice Fadel, Ragi Ghosn, Flavia Khatounian

► **To cite this version:**

Charbel Zaghrini, Gabriel Khoury, Maurice Fadel, Ragi Ghosn, Flavia Khatounian. On-line loss and global efficiency simulation tool for electric vehicles applications. IECON 2021 – 47th Annual Conference of the IEEE Industrial Electronics Society, Oct 2021, Toronto, Canada. hal-03549587

**HAL Id: hal-03549587**

**<https://ut3-toulouseinp.hal.science/hal-03549587v1>**

Submitted on 31 Jan 2022

**HAL** is a multi-disciplinary open access archive for the deposit and dissemination of scientific research documents, whether they are published or not. The documents may come from teaching and research institutions in France or abroad, or from public or private research centers.

L'archive ouverte pluridisciplinaire **HAL**, est destinée au dépôt et à la diffusion de documents scientifiques de niveau recherche, publiés ou non, émanant des établissements d'enseignement et de recherche français ou étrangers, des laboratoires publics ou privés.

# On-line loss and global efficiency simulation tool for electric vehicles applications

Charbel Zaghrini  
*ESIB, CINET, Faculté d'Ingénierie*  
*Université Saint-Joseph de Beyrouth*  
Beirut, Lebanon  
charbel.zaghrini@net.usj.edu.lb

Gabriel Khoury  
*ESIB, CINET, Faculté d'Ingénierie*  
*Université Saint-Joseph de Beyrouth*  
Beirut, Lebanon  
gabriel.khoury@usj.edu.lb

Maurice Fadel  
*LAPLACE, Université de Toulouse*  
*CNRS, INPT, UPS*  
Toulouse, France  
maurice.fadel@laplace.univ-tlse.fr

Ragi Ghosn  
*ESIB, CINET, Faculté d'Ingénierie*  
*Université Saint-Joseph de Beyrouth*  
Beirut, Lebanon  
ragi.ghosn@usj.edu.lb

Flavia Khatounian  
*ESIB, CINET, Faculté d'Ingénierie*  
*Université Saint-Joseph de Beyrouth*  
Beirut, Lebanon  
flavia.khatounian@usj.edu.lb

**Abstract**— This paper is dedicated to control-based energy optimization tools useful for the electric vehicles (EVs) propulsion chain, which puts in interaction an electric motor and its energy source static converter. It is essential in energy optimization studies to take into account all possible losses of the propulsion chain components according to the operating point. For that reason, the present work provides an accurate loss analysis solution, by studying the various elements losses of an electric traction chain motorized by an Electrically-Excited Synchronous Motor (EESM). The machine power balance is established while taking copper and iron losses into account. Moreover, the inverter and chopper losses and efficiencies are evaluated using a novel technique that consists in creating a modified version of output voltages affected by the converters losses. Finally, all losses data are gathered in order to simulate the system on-line losses distribution and global efficiency for different operating conditions.

**Keywords**—EESM, iron losses, converter losses, power balance, on-line losses simulation, global efficiency

## I. INTRODUCTION

Energy efficiency optimization has become a main scope of recent researches in order to promote sustainable energies and reduce its consumption. EVs applications are the most attractive in that matter, being considered the most viable eco-friendly solution for transportation systems. The traction elements losses knowledge is thus an essential aspect in operating the electric drive system energy efficiently. When it comes to the electric motor, which is the main element in an EV propulsion chain, iron losses are classified as one of the most relevant losses in it, especially at high speeds in flux weakening regions. Conventionally, most authors take account of iron losses in the electric Park equations by modifying the machine electric circuit, where they are represented by an equivalent resistor which value needs experimental identification [1]. A mechanical analogy is adopted in order to estimate these losses without having to deal with the mentioned coefficient, where iron losses are considered as mechanical losses that tend to reduce the electromagnetic torque [2].

Another key component in EVs propulsion chain is the power converter which consists of an inverter feeding the stator phases and a chopper feeding the excitation coil. The semi-conductors used in these devices introduce considerable conduction and switching losses, especially at certain working temperatures and switching frequencies [3]. It is therefore advantageous to take the dynamic and thermal aspects of the

converters components in the loss analysis and that the loss model can be used in an algebraic optimization procedure. Circuit-averaging is a popular method used in this domain but can present some difficulties in correctly defining the right variables to average [4]. Another approach consists in using a state-space average model [5] and is applied on an ordinary differential equation which explicitly represents the system equations. This method has a solid mathematical basis but fails to distinguish fast state variables from slow state ones. Multiple researches have been conducted in order to provide a loss simulation tool for electric vehicles applications using popular simulation platforms such as Matlab/Simulink and PSIM. In [6], a loss analysis simulation model is designed using a co-simulation concept linking the PSIM schematic to the Simulink one, to analyze the efficiency of an on-board charger (OBC) by evaluating its semi-conductors losses and inductors/transformers magnetic losses. The method can be applied to various converter applications such as traction ones but the machine loss modelling is still required for a complete drive chain loss analysis. A research in [7] presents another loss simulation tool for EVs drive system where the inverter and machine losses were simulated separately without treating the global system efficiency, and an experimental identification was needed in order to approximate the machine iron losses.

In this paper, a complete loss analysis is conducted on the main elements of an EV drive system motorized by an EESM. All losses are gathered in Matlab/Simulink in order to create a loss simulation tool that allows the user to have an on-line visualization of the machine, inverter and chopper losses, along with the system global efficiency at any desired working point. The converter losses in the proposed model are validated using PSIM thermal module, so that near realistic results are consolidated in one single platform. To begin with, all the machine losses are evaluated while taking iron losses into account in the mechanical equation so that the experimental identification of the equivalent resistor is avoided. After that, the converter losses are precisely exploited using a hybrid average model strategy based on bond graphs [8] to correctly manage causality errors and Petri networks to precisely represent the different converter states [9], solving the fore mentioned issues in [4] and [5]. Furthermore, the manufacturer characteristics representing the semi-conductors voltage drops and dissipated energies at a specific working temperature are also implemented in the analysis in order to take the components thermal aspect into consideration. Finally, a novel method that consists in creating a modified version of the converter output voltages is

used to calculate the converter power balance and global efficiency.

## II. ELECTRICALLY-EXCITED SYNCHRONOUS MOTOR LOSS MODEL

Apart from the saturation phenomena, a model based on circuit equations is usually sufficient for simulation purposes as it brings acceptable precision with short simulation times. In this section, the power balance of an EESM is developed using Park equations, while taking iron losses into account.

### A. EESM Park model

The salient pole EESM Park model using Concordia transform is detailed in (1)-(7) :

- Stator electrical equations

$$v_d = (R_s + L_d s) i_d - L_q \omega_r i_q + M s i_r \quad (1)$$

$$v_q = (R_s + L_q s) i_q + L_d \omega_r i_d + M \omega_r i_r \quad (2)$$

- Stator flux equations

$$\varphi_d = L_d i_d + M i_r \quad (3)$$

$$\varphi_q = L_q i_q \quad (4)$$

- Rotor electrical equations

$$v_r = (R_r + L_r s) i_r + M s i_d \quad (5)$$

- Mechanical equations

$$f \Omega_r + J \frac{d\Omega_r}{dt} = T_{em} - T_l \quad (6)$$

$$T_{em} = M p i_q i_r + (L_d - L_q) p i_d i_q \quad (7)$$

The variables and parameters appearing in this model are listed down below:

- $v_d, v_q$  : direct and quadrature axis stator voltages,
- $v_r$  : excitation rotor coil voltage,
- $i_d, i_q$  : direct and quadrature axis stator currents,
- $i_r$  : excitation rotor coil current,
- $R_s, R_r$  : stator and rotor resistance,
- $L_d, L_q$  : direct and quadrature axis stator inductances,
- $L_r$  : rotor inductance,
- $M$  : stator and rotor mutual inductance,
- $\omega_r$  : electrical rotor velocity,
- $s$  : Laplace operator,
- $\Omega_r$  : mechanical rotor velocity,
- $J$  : total motor load inertia,
- $f$  : viscous friction coefficient,
- $p$  : pair of poles number,
- $T_{em}$  : electromagnetic torque,
- $T_l$  : load torque.

### B. Iron losses modelling

Giorgio Bertotti developed in the 1980s an accurate iron losses model [10], by dividing it into the three main types of losses: hysteresis losses due to the hysteresis magnetizing cycle experienced by the metal sheet, eddy currents losses due to excitation field variation inside the material, and the so-called excess losses appearing at high frequencies due to induced microscopic currents

Giorgio Bertotti's iron losses model is described as in (8):

$$P_{Fe} = k_H \omega_r \cdot \hat{\varphi}^2 + k_F \omega_r^2 \cdot \hat{\varphi}^2 + k_e \omega_r^{3/2} \cdot \hat{\varphi}^{3/2} \quad (8)$$

where:

- $P_{Fe}$  : iron losses power,
- $\hat{\varphi}$  : amplitude of the stator magnetic flux,
- $k_H$  : coefficient representing hysteresis losses,
- $k_F$  : coefficient representing eddy current losses,
- $k_e$  : coefficient representing excess losses.

The amplitude of the stator magnetic flux can be calculated as follows:

$$\hat{\varphi} = \sqrt{\varphi_d^2 + \varphi_q^2} \quad (9)$$

In this study, iron losses are considered as mechanical losses rather than copper ones, which tend to reduce the electromagnetic torque. Consequently, they will be represented by an additional resistive torque in the mechanical equation as in (10):

$$T_{Fe} = \frac{P_{Fe}}{\Omega_r} \quad (10)$$

The modified mechanical equation taking into account iron losses is described in (11):

$$f \Omega_r + J \frac{d\Omega_r}{dt} = T'_{em} - T_l \quad (11)$$

where  $T'_{em} = T_{em} - T_{Fe}$  is the electromagnetic torque affected by the iron losses representative torque.

### C. EESM power balance

The EESM power balance listed in (12)-(16) is obtained using the electrical equations in (1)-(5). It should be noted that iron losses will not appear in the below list since they were integrated in the mechanical equation instead of the electrical ones.

$$P_{el_s} = v_d i_d + v_q i_q \quad (12)$$

$$P_{el_r} = v_r i_r \quad (13)$$

$$P_{J_s} = R_s (i_d^2 + i_q^2) \quad (14)$$

$$P_{J_r} = R_r i_r^2 \quad (15)$$

$$P_{em} = \omega_r (\varphi_d i_q + \varphi_q i_d) \quad (16)$$

Friction losses ( $P_f$ ) and mechanical output power ( $P_{mec}$ ) can also be calculated using (17) and (18) respectively:

$$P_f = f \Omega_r^2 \quad (17)$$

$$P_{mec} = T_l \Omega_r \quad (18)$$

where:

- $P_{el_s}, P_{el_r}$  : stator and rotor input electrical power,
- $P_{J_s}, P_{J_r}$  : stator and rotor Copper losses,
- $P_{mag}$  : magnetic power stored in the air-gap,
- $P_{em}$  : electromagnetic power.

Since iron losses were taken into account in the machine model, the electromagnetic power in (16) will be affected by these losses, and therefore will be calculated as in (19):

$$P'_{em} = P_{el,s} + P_{el,r} - P_{j_s} - P_{j_r} - P_f - P_{Fe} \quad (19)$$

where  $P'_{em}$  is the final electromagnetic output power.

Fig. 1 shows a block diagram explaining the machine modelling technique used while taking iron losses into consideration. Each section associated power elements are also represented.

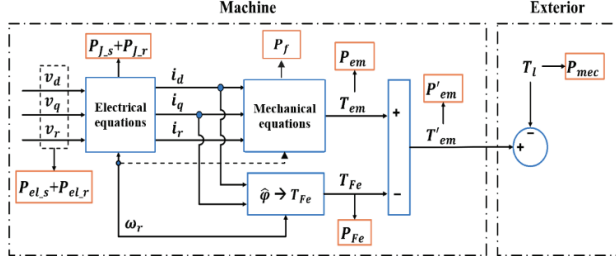


Fig. 1. Block diagram of the machine modelling technique with iron losses consideration.

### III. INVERTER LOSSES MODELLING

A single inverter arm is used for modelling purposes as shown in Fig. 2, where the average output voltage is marked with other important variables such as the load current and the battery current and voltage. Cabling inductances are not taken into consideration in order to discern the components different conduction phases and deduce the functionality of an inverter arm [8],[9].

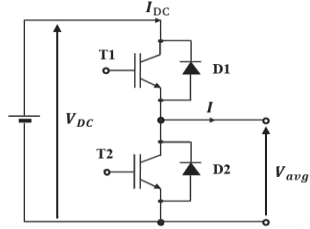


Fig. 2 Diagram of an inverter arm

The voltage  $V_{DC}$  is delivered by the battery while the current  $I$  is imposed by the load.  $I_{DC}$  and  $V_{avg}$  are the DC link current and average voltage respectively. By designating  $\rho$  the duty cycle defined by the Pulse Width Modulation (PWM) technique and  $\rho_d$  the ratio of dead-time to cutting period, the inverter average voltage affected by inverter losses and transistors dead-time can be defined over a switching period as in (20) and (21):

- $I \geq 0$

$$V_{avg} = \left(\rho - \frac{\rho_d}{2}\right) \cdot [V_{DC} - V_{ce}(I)] + \left(1 - \left(\rho - \frac{\rho_d}{2}\right)\right) \cdot [-V_d(I)] \quad (20)$$

- $I < 0$

$$V_{avg} = \left(\rho + \frac{\rho_d}{2}\right) \cdot [V_{DC} + V_d(|I|)] + \left(1 - \left(\rho + \frac{\rho_d}{2}\right)\right) \cdot [V_{ce}(|I|)] \quad (21)$$

Where:

- $V_{ce}$  : transistors collector-emitter voltage,
- $V_d$  : diodes threshold voltage.

Transistors collector-emitter voltages and diodes threshold voltages vary in function of the load current and their characteristics for specific junction temperatures are given by the manufacturer. The models in (22) and (23) allow to precisely interpolate these electrical quantities. The interpolation results of the MITSUBISHI 6MBP300RA060 semi-conductors voltage drop characteristics at a 125°C gate temperature are shown in Fig. 3.

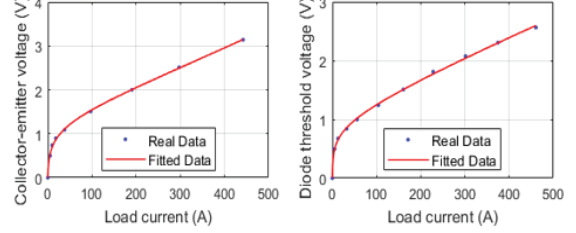


Fig. 3 Collector-emitter voltage (left) and diode threshold voltage (right) characteristics interpolation

- Transistor

$$V_{ce}(I) = V_{ce_{k1}} \ln\left(1 + \frac{I}{V_{ce_{k2}}}\right) + V_{ce_{k3}} I + V_{ce_{k4}} I^2 \quad (22)$$

- Diode

$$V_d(I) = V_{d_{k1}} \ln\left(1 + \frac{I}{V_{d_{k2}}}\right) + V_{d_{k3}} I + V_{d_{k4}} I^2 \quad (23)$$

where:

- $V_{ce_{k1}}, V_{ce_{k2}}, V_{ce_{k3}}, V_{ce_{k4}}$  : collector-emitter voltage drop static law coefficients,
- $V_{d_{k1}}, V_{d_{k2}}, V_{d_{k3}}, V_{d_{k4}}$  : diode voltage drop static law coefficients.

Losses in an inverter can be divided into conduction ( $P_{inv,cond}$ ) and switching losses ( $P_{inv,sw}$ ). Conduction losses are sensitive to the voltage drops across the semi-conductors terminals and the current passing through the latter. On the other hand, switching losses depend on the dissipated energy between the transistors change of states. These losses are proportional to the converter switching frequency. Furthermore, diodes reverse recovery energy is also dissipated into the transistors due to the diode recovery time but this phenomenon is neglected in the current analysis. The loss model equations can be defined as follows:

- $I \geq 0$

$$P_{T_1} = \rho V_{ce}(I) I + \{k_{E_{on}} E_{on}(I) + k_{E_{off}} E_{off}(I)\} \cdot f_{sw} \quad (24)$$

$$P_{D_2} = (1 - \rho) V_d(I) I \quad (25)$$

$$P_{inv,cond} = \rho V_{ce}(I) I + (1 - \rho) V_d(I) I \quad (26)$$

$$P_{inv,sw} = \{k_{E_{on}} E_{on}(I) + k_{E_{off}} E_{off}(I)\} \cdot f_{sw} \quad (27)$$

- $I < 0$

$$P_{T_2} = (1 - \rho) V_{ce}(|I|) |I| + \{k_{E_{on}} E_{on}(|I|) + k_{E_{off}} E_{off}(|I|)\} \cdot f_{sw} \quad (28)$$

$$P_{D_1} = \rho V_d(|I|) |I| \quad (29)$$

$$P_{inv\_cond} = (1 - \rho)V_{ce}(|I|)|I| + \rho V_d(|I|)|I| \quad (30)$$

$$P_{inv\_sw} = \{k_{E_{on}}E_{on}(|I|) + k_{E_{off}}E_{off}(|I|)\} \cdot f_{sw} \quad (31)$$

where:

- $P_{T_1}, P_{T_2}$  : T1 and T2 conduction and commutation losses,
- $P_{D_1}, P_{D_2}$  : D1 and D2 conduction losses,
- $f_{sw}$  : inverter switching frequency,
- $E_{on}, E_{off}$  : ON and OFF states dissipated energies,
- $k_{E_{on}}, k_{E_{off}}$  : ON and OFF states corrective factors.

The dissipated energies characteristics at ON and OFF states given by the manufacturer can be interpolated using the same models adopted for voltage drops representation in (22) and (23). The corrective factors are the ratio of the battery voltage used in simulations over the voltage used by the manufacturer while testing the dissipated energies at ON and OFF states. The inverter total losses can be expressed as in (32):

$$P_{inv\_losses} = P_{T_1} + P_{T_2} + P_{D_1} + P_{D_2} \quad (32)$$

A modified version of inverter output voltages (i.e. stator input voltages) affected by its losses is created from the average voltages developed in (20)(21), using the model in (33).

$$\begin{bmatrix} v'_a \\ v'_b \\ v'_c \end{bmatrix} = \frac{1}{3} \begin{bmatrix} 2 & -1 & -1 \\ -1 & 2 & 1 \\ -1 & -1 & 2 \end{bmatrix} \cdot \begin{bmatrix} V_{avg(a)} \\ V_{avg(b)} \\ V_{avg(c)} \end{bmatrix} \quad (33)$$

Where  $V_{avg(a)}, V_{avg(b)}, V_{avg(c)}$  and  $v'_a, v'_b, v'_c$  represent the three phases average voltages and modified stator voltages respectively, affected by the inverter losses.

This new approach presents multiple advantages. The first one consists in that the system is simulating realistic machine voltages affected by the inverter losses, and the other one is that through these voltages, the inverter input power leading to its power balance can be created by simply adding the inverter losses ( $P_{inv\_losses}$ ) to the inverter output power (stator input power) as shown in (34). This is justified by the fact that the modified voltages will also affect the machine currents by the inverter losses ( $i'_a, i'_b, i'_c$ ) which leads its output power (shown in (12)) to be also affected by the latter.

$$P_{inv\_input} = P_{el\_s} + P_{inv\_losses} \quad (34)$$

The produced model in Matlab-Simulink is validated by comparing the simulation results of the inverter losses to those obtained using PSIM software, which uses a reliable model of electronic components by taking more precisely into account the manufacturer datasheets. A DC voltage of 400 V is applied with a 3 phase voltage reference amplitude of 230 V and a load current of 200 A. PSIM and Matlab simulation results are shown in Fig. 4 (A) and Fig. 4 (B), where the diodes and transistors conduction losses are plotted in red and blue respectively, the transistors switching losses in green and the inverter total losses in purple. Their average values in Watts are also marked on the graphs.

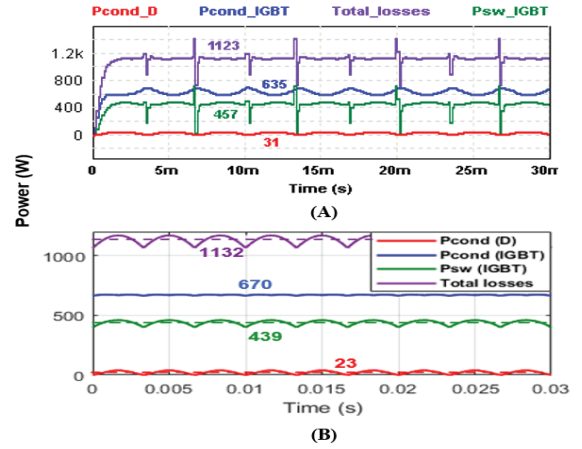


Fig. 4 Inverter losses simulation using PSIM (A) and Matlab (B)

The above results validate the proposed loss modelling technique since the average losses values obtained from Matlab are very close to those obtained from PSIM. The small differences are due to the interpolation accuracy of the components characteristics and are considered negligible when compared to the total electrical power.

#### IV. CHOPPER LOSSES MODELLING

The same one leg inverter electronic circuit (Fig. 2) and average modelling procedure is adopted for chopper loss modelling as it gives the same output results for the conventional buck/boost circuits. The main differences reside in the following points:

- The excitation load current is a unidirectional DC current, therefore only the upper transistor and the lower diode will be switching.
- Transistors dead-time does not exist since real chopper electronic circuits do not have short-circuit capabilities.
- The semi-conductors are less powerful since the rated current/voltage values of the excitation coil are lower than those of the stator coils.
- The average excitation voltage signal is the same as the normal one since they are DC quantities.

Fig. 5 shows the diagram of an inverter arm equivalent to a chopper circuit. The voltage  $V_{DC}$  is delivered by the same battery used to feed the inverter while the direct current  $I_{exc}$  is imposed by the excitation load.  $I_{ch}$  and  $V_{exc}$  are the chopper DC link current and average excitation voltage respectively.

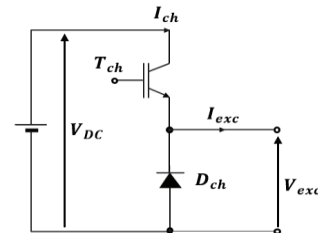


Fig. 5 Diagram of an inverter arm equivalent to a chopper circuit

Considering  $v^*_r$  the control reference excitation voltage, the transistor duty cycle can be calculated as in (35):



$$\rho_{ch} = \frac{v'_r}{V_{DC}} \quad (35)$$

The chopper average voltage affected by its components losses can be defined over a switching period as in (36):

$$V_{exc} = \rho_{ch} \cdot [V_{DC} - V_{ce\_ch}(I_{exc})] + (1 - \rho_{ch}) \cdot [-V_{d\_ch}(I_{exc})] \quad (36)$$

The average chopper voltage is compared to a positive triangular carrier signal of frequency  $f_{sw\_ch}$  and amplitude  $V_{DC}$  in order to create the modified rotor voltage affected by chopper losses ( $v'_r$ ) which induces a modified rotor current ( $i'_r$ ) in the excitation coil. The chopper losses model equations including conduction ( $P_{ch\_cond}$ ) and switching losses ( $P_{ch\_sw}$ ) are defined as follows:

$$P_{T\_ch} = \rho_{ch} V_{ce\_ch}(I_{exc}) I_{exc} + \left\{ k_{E_{on\_ch}} E_{on\_ch}(I_{exc}) + k_{E_{off\_ch}} E_{off\_ch}(I_{exc}) \right\} \cdot f_{sw\_ch} \quad (37)$$

$$P_{D\_ch} = (1 - \rho_{ch}) V_{d\_ch}(I_{exc}) I_{exc} \quad (38)$$

$$P_{ch\_cond} = \rho_{ch} V_{ce\_ch}(I_{exc}) I_{exc} + (1 - \rho_{ch}) V_{d\_ch}(I_{exc}) I_{exc} \quad (39)$$

$$P_{ch\_sw} = \left\{ k_{E_{on\_ch}} E_{on\_ch}(I_{exc}) + k_{E_{off\_ch}} E_{off\_ch}(I_{exc}) \right\} \cdot f_{sw\_ch} \quad (40)$$

where:

- $P_{T\_ch}$  : chopper transistor conduction and switching losses,
- $P_{D\_ch}$  : chopper diode conduction losses,
- $f_{sw\_ch}$  : chopper switching frequency,
- $V_{ce\_ch}$  : collector-emitter voltage of the chopper transistor,
- $V_{d\_ch}$  : threshold voltage of the chopper diode,
- $E_{on\_ch}, E_{off\_ch}$  : ON and OFF states chopper dissipated energies,
- $k_{E_{on\_ch}}, k_{E_{off\_ch}}$  : ON and OFF states chopper corrective factors.

The chopper power balance (losses, output and input power) is developed in the following:

$$P_{ch\_losses} = P_{T\_ch} + P_{D\_ch} \quad (41)$$

$$P_{ch\_output} = P_{el\_r} = v_r i_r \quad (42)$$

$$P_{ch\_input} = P_{ch\_output} + P_{ch\_losses} \quad (43)$$

## V. SIMULATION RESULTS OF THE PROPOSED TOOL

The MATLAB implementation of the loss simulation tool is summarized in Fig. 6, where each section losses are marked in red, control blocks in blue, and the converters with their respective voltages modification in orange. The current references were calculated using the minimum current per torque (minCPT) strategy [11]. The latter takes a torque reference as input and calculates the corresponding current references ( $i^*_d, i^*_q, i^*_r$ ) using the Lagrangian multiplier method, which has an objective of determining the minimum of the trio currents that satisfies (7) for a certain torque reference.

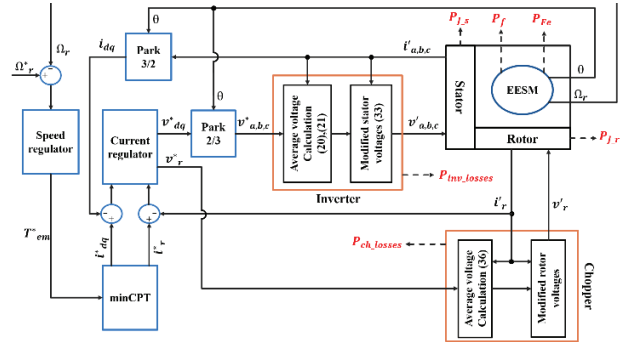


Fig. 6 Schematic block diagram showing the MATLAB implementation of the loss simulation tool

The inverter and chopper respective conduction and switching losses are added together for simulation purposes in order to create the converter total conduction and switching losses as shown in (44) and (45):

$$P_{cond} = P_{inv\_cond} + P_{ch\_cond} \quad (44)$$

$$P_{sw} = P_{inv\_sw} + P_{ch\_sw} \quad (45)$$

The traction chain total losses and global efficiency are expressed as in (46) and (47) respectively:

$$P_{total\_losses} = P_{J_s} + P_{J_r} + P_{Fe} + P_f + P_{cond} + P_{sw} \quad (46)$$

$$Eff = \frac{P_{mec}}{P_{mec} + P_{total\_losses}} \quad (47)$$

The on-line losses and global efficiency results of the proposed simulation tool are shown on four operating points, chosen in the following manner:

- Point A: Low speed / Low torque (300 rpm – 24 N.m)
- Point B: Low speed / High torque (300 rpm – 220 N.m)
- Point C: High speed / High torque (2300 rpm – 220 N.m)
- Point D: High speed / Low torque (4000 rpm – 24 N.m)

These operating points are chosen inside the limit envelope curve in the torque/speed domain shown in Fig. 7. For each torque value the associated speed limit corresponds to the maximum voltage given by the inverter, calculated using the MinCPT strategy. Fig. 8 shows the propulsion chain losses distribution and global efficiency when the machine is operating at point A, using the proposed tool. The machine, inverter and chopper parameters used in simulations are found in the Appendix.

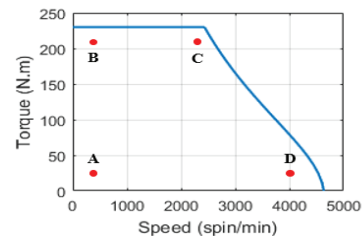


Fig. 7 Operating points chosen inside the minCPT speed/torque limit envelope curve

## VII. APPENDIX

The EESM, inverter and chopper specifications are listed in the following:

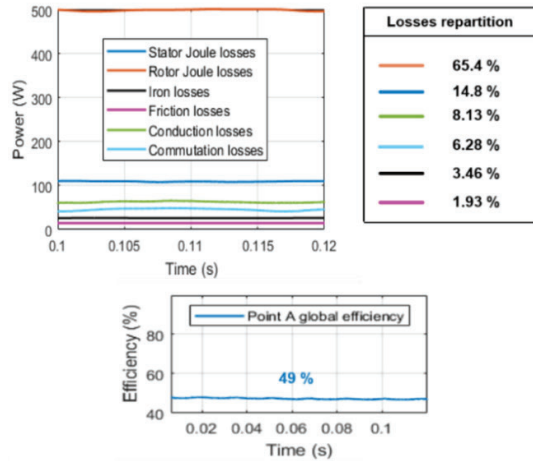


Fig. 8 Propulsion chain elements real-time losses distribution and global efficiency at point A

The results shown in Fig. 8 are grouped in Table 1 for each operating point specified in Fig. 7.

Table 1 Propulsion chain real-time losses (in Watts) and global efficiency (in %) at each operating point

Point	$P_{J,s}$	$P_{J,r}$	$P_{Fe}$	$P_f$	$P_{cond}$	$P_{sw}$	Eff
A	94	485	26	15	58	44	49
B	9082	485	90	15	1202	306	37
C	10180	485	4552	870	1352	322	75
D	144	485	4721	2632	79	51	92

The proposed loss simulation tool will therefore be used in future works to optimize the EESM energy efficiency by acting on the control. Table 1 shows that the proposed tool allows to identify operating points with higher efficiency, the most relevant losses at a specific working point, and the losses evolution depending on the operating conditions. It therefore allows to test the effectiveness of energy optimization algorithms on all the traction chain elements. Moreover, it is clear that the converter losses can be significant in certain operating conditions (points B and C) so it would be advantageous to take these losses into consideration in the optimization procedure.

## VI. CONCLUSION

In this paper, a general loss analysis simulation tool dedicated to EVs applications was presented, with the aim of bringing benefits to the energy efficiency optimization domain. The machine upon which the study was conducted is the EESM, which gained a lot of attention in the electric vehicles market. The machine power balance was established while taking iron losses into account in the mechanical equation. Furthermore, the inverter and chopper losses were evaluated using the converter average model, taking into account the switching components voltage drops and dissipated energies in the loss model, which was validated using PSIM software. Finally, all losses data were gathered into a simulation tool that allows an on-line visualization of the EV drive system total losses and global efficiency at different operating conditions. The results shown are those obtained with a MinCPT-type control strategy, which will be modified according to the desired operating point in future energy optimization works conducted on the EESM.

EESM	
Rated power	50 kW
Rated torque	230 N.m
Rated speed	2000 rpm
Rated stator voltage	230 V
Rated rotor voltage	400 V
Rated rotor current	5 A
Inverter	
DC bus voltage	400 V
Switching frequency	8 kHz
Semi-conductors	6MBP300RA060
Chopper	
DC bus voltage	400 V
Switching frequency	3 kHz
Semi-conductors	SKM50GB-123D

## VIII. REFERENCES

- [1] G. Khoury, R. Ghosn, F. Khatounian, M. Fadel, M. Tientcheu. *An Energy Efficient Scalar Control Taking Core Losses into Account*. COMPEL - The International Journal for Computation and Mathematics in Electrical and Electronic Engineering, vol. 37, no. 2, 2018.
- [2] G. Khoury, R. Ghosn, F. Khatounian, M. Fadel, M. Tientcheu. *Including core losses in induction motors dynamic model*. 3<sup>rd</sup> International Conference on Renewable for Developing Countries (REDEC), Zouk Mosbeh, Lebanon, 2016, pp. 1-6.
- [3] H. H. Bao, W. Zhang, Y. Yang and Y. Chen. *Calculation and analysis of IGBT power loss in drive system for EV*. IEEE International Conference on Applied Superconductivity and Electromagnetic Devices (ASEMD), Shanghai, China, 2015, pp. 276-277.
- [4] Middlebrook, Cuk. *A general unified approach to modeling switching converters power stage*. International Journal of Electronics, 1977, Vol.42, n<sup>o</sup>. 6, pp. 521-550.
- [5] P.T. Krein, J. Bentsman, R.M. Bass and B.L. Lesieutre. *On the Use of Averaging for the Analysis of Power Electronics Systems*. IEEE transaction on Power Electronics, 1990, Vol. 5, n<sup>o</sup>. 2, pp. 182-190.
- [6] Won-Yong Sung, Dong-Gyun Woo, Yun-Sung Kim, Bong-Gi You and Byoung-Kuk Lee. *Advanced simulation model for loss analysis of converters in electric vehicles*. 2012 IEEE Vehicle Power and Propulsion Conference, Seoul, Korea (South), 2012, pp. 1206-1210.
- [7] Q. K. Nguyen and J. Roth-Stielow. *Analysis and Modelling of the Losses for the Electrical Drive System of an Electric Vehicle*. 2014 IEEE Vehicle Power and Propulsion Conference (VPPC), Coimbra, Portugal, 2014, pp.
- [8] B. Allard, H. Morel, Ph. Lautier, J.M. Rétif. *Bond Graphs for Average Modeling of Power Electronics Converters*. SCS Simulation Series, 1997, Vol. 29, N<sup>o</sup>. 1, pp. 201-206.
- [9] B. Allard, H. Morel and J.P. Chante. *Power Electronics Circuit Simulation Using Bond Graph and Petri Network Techniques*. Proceedings of IEEE PESC'93 - Seattle USA, 1993, pp. 5-12.
- [10] Giorgio BERTOTTI. *General properties of power losses in soft ferromagnetic materials*. IEEE Transactions on magnetics, 24(1):621-630, 1988.
- [11] Mingming Huang, Quanzhen Huang, Yang Zhang, Xinjun Guo. *A Comprehensive Optimization Control Method for Hybrid Excitation Synchronous Motor*. Mathematical Problems in Engineering, vol. 2020, Article ID 1390650, 11 pages, 2020.